AN EXPERIMENTAL STUDY OF CHITOSAN WET SPINNING PROCESS

Alin Alexandru ENACHE[1], Laurent DAVID[2], Jean-Pierre PUAUX[3], Ionut BANU[4], Grigore BOZGA[5]

This work investigates, mainly from modelling point of view, the process of chitosan fibers formation by coagulation from aqueous solution using sodium hydroxide solution as coagulant (wet spinning). The experimental data were obtained using a spinning laboratory plant. The modelling and simulation study of the chitosan hydrogel wet-spinning conducted to results in an acceptable concordance with the measured data on a laboratory unit. This is proving that the proposed model can be used in the calculation of the coagulation step of the fiber formation process by wet spinning.

Keywords: chitosan, wet spinning, biopolymers, fibers, mathematical modelling

1. Introduction

The chitosan is a derived polysaccharide from chitin. After cellulose, chitin is considered the second most abundant polysaccharide in the world. The difference between chitin and chitosan consists in the possibility of solubilizing a polymer in diluted acid medium. In this condition the chitin is insoluble, while the chitosan is soluble (Fig. 1). The border between chitin and chitosan can be traced around 60% of degree of acetylation (DA) [1]. Other authors are considering this border situated at a DA 50%. A polymer with a DA less than 50% is called chitin and a polymer with DA greater than 50% is called chitosan [2]. However, this border is influenced by several parameters such as the degree of polymerization, the copolymer obtaining process [3-5], the distribution of acetyl units [6], the pH and the ionic strength of the solution [7]. In practice, the chitosan usually refers to a family of polymers derived from chitin, obtained by deacetylation, rather than a well-defined compound [8].

Chitosans have properties such as biodegradability, biocompatibility, low toxicity, antimicrobial activity [9]. They can be processed in a variety of forms

[1] PhD Student, Dep. of Chemical and Biochemical Engineering, University POLITEHNICA of Bucharest, Romania, e-mail: a_enache@chim.upb.ro
[2] Prof., Laboratoire Ingénierie des Matériaux Polymères (IMP), Université Lyon 1, Lyon, France e-mail: laurent.david@univ-lyon1.fr
[3] Prof., Laboratoire Ingénierie des Matériaux Polymères (IMP), Université Lyon 1, Lyon, France e-mail: jean-pierre.puaux@univ-lyon1.fr
[4] Lecturer, Dep. of Chemical and Biochemical Engineering, University POLITEHNICA of Bucharest, Romania, e-mail: i_banu@chim.upb.ro
[5] Prof., Dep. of Chemical and Biochemical Engineering, University POLITEHNICA of Bucharest, Romania, e-mail: g_bozga@chim.upb.ro

such us hydrogels, micro and nanoparticles [10,11], solutions [12], membranes or multimembrane hydrogels [13], as well as nanofibers [14, 15], yarns [16,17], films [18] etc.

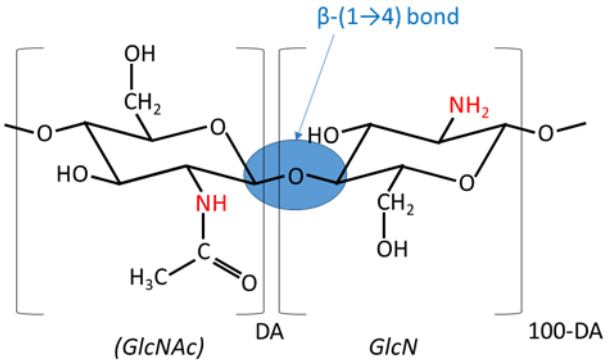

Fig. 1 Chemical structure of chitin and chitosan; GlcNAc represent glucopyranose acetamido unit and GlcN is glucopyranose amino unit, DA is the degree of acetylation.

The chitosan and its derivatives are today used or envisaged in many fields of application: agriculture [19], packaging [20], adhesives [21], textile industry [22], cosmetic products [23], separation technologies [24] and biomedical [25,26]. In the biomedical field, chitosan can be used for tissue engineering [27-29], vectorization of the active principles [30-32] or for other technologies such as bioimaging [33] or biosensors [34]. The mechanism of chitosan coagulation is very complex and not fully proven. This involves many parameters such as polymer concentration, degree of acetylation, average molecular weight, the nature of coagulation agent, concentration of coagulation agent, temperature of the coagulation bath.

Chitosan is soluble in acid and alkaline solutions [35,36]. The most used solubilization agent is the acetic acid. The acid is added in stoichiometric amount in order to protonate the amino groups of the chitosan molecule. According to Rinaudo [37] the pH of the acid polymer solution should be between 4.5 and 5. Chenite et al. [38] reported that the chitosan remains in solution until the pH is under 6.2; over this pH, the first crystals of chitosan are starting to appear. The range of pH necessary for neutralization of $-NH_3^+$ groups is between 6.2 and 7.4. The most used base for chitosan coagulating is sodium hydroxide. The mechanism of chitosan coagulation can be resumed such as equation (1) describes the mechanism of chitosan coagulation (Ch a chitosan molecule:

$$Ch-NH_2 \xrightarrow[H_2O+CH_3COOH]{solubilisation} Ch-NH_3^{\oplus}CH_3COO^{\ominus} \xrightarrow[NaOH]{coagulation} Ch-NH_2+CH_3COO^{\ominus}Na^{\oplus} \quad (1)$$

The first studies for the chitosan spinning was made by Rigby [39], who dissolved 3.8% (w/w) of the polymer in 1.2% aqueous solution of acetic acid. The

result is an extrusible solution (named collodion). The fibers were obtained by extrusion of collodion in a coagulation bath consisting of 93% water, 4.6% of sodium acetate, 2% sodium hydroxide and 0.2% sodium dodecyl sulfate followed by washing and drying under tension.

Other spinning tests have been reported by Ming [40], who dissolved the 0.5% solution of acetic acid in order to obtain a collodion with 5-6 % (w/v). The coagulation bath contained 100 parts water, 2 to 2.5 parts NaOH, 15 parts glycerin and an undescribed amount of sodium sulfate. He added to the collodion 2 parts of zinc acetate, 4 of glycerin and 0.5 of alcohol to improve its stability. The chitosan wet spinning process implies several stages. The first is the solubilization of the chitosan (the obtained solution is called "collodion) followed by the passing of the collodion through the immersed spinneret in the coagulation bath. The spinning collodion starts to coagulate during the passage in the coagulation bath. The next step is the washing (removing the coagulation agent) of the filament followed by the drying of the filament in order to eliminate the contained liquid. Finally, the fiber is reeling on a reel.

2. Experimental

2.1 Materials

The chitosan used in this work was purchased from Mahtani Chitosan (batch type: 114) having the characteristics presented in Table 1. Sodium hydroxide and glacial acetic acid were bought from Carlo Erba Reagents bold.

The wet spinning experiments were performed with chitosan solution having the concentration 2.5 % (w/w) and sodium hydroxide solutions with concentration 1.5 (mol/L).

Table 1

Chitosan characteristics

Number-average molar mass of chitosan ($\bar{M}_n$)	397 ± 10 kg/mol
Weight-average molar mass of chitosan ($\bar{M}_w$)	547 ± 10 kg/mol
Solid chitosan density	1200 kg/m^3
Water content in chitosan powder	7 ± 0.5 wt%
Degree of acetylation	2.82 ± 0.5 %
Number of 'amino' groups per chitosan chain ($n_{NH_3^+}$)	2340 groups /molecule

2.2 Method

The first step was the chitosan purification. The chitosan was dissolved at 0.5 wt% in the presence of stoichiometric amount of acetic acid necessary to protonate the amino groups. The solution was kept under mixing for one night to be ensured that all chitosan was dissolved. Then the solution was filtered successively on 3, 0.80 and 0.45 μm cellulose acetate membranes using a column

with compressed air working at 3 bars. Next, ammonia solution was added up until the pH was 9 in order to precipitate all the chitosan. Then repeatedly washed with deionized water and centrifuged until the pH was neutral. Finally, the precipitate chitosan was immersed in freezer for one night and then immersed and left for three days in dry freezer. During this stage, the chitosan was freeze drying.

The second step was to prepare the chitosan solution ~2.5 wt%. In this aim 12.5 grams of chitosan were weighted, and 550 mL water was added (the volume of water should be in excess (~10%) in order to compensate the water evaporation during the mixing). These were added into a vessel provided with mechanical mixing. Finally, a stoichiometric volume of glacial acetic acid was added (4.12 mL) in order to protonate the amino sites in accordance with the degree of acetylation. The solution was kept at room temperature under mixing (50 rpm) over the night (approximately 18 hours). Next, the obtained chitosan solution (collodion) was centrifuged for 10 minutes at 5000 rpm, in order to eliminate the air bubbles.

The injection system consists of a piston which descends into chitosan vessel forcing the chitosan dope solution to pass through a silicon hose. On the dope chitosan solution pathway towards the mechanical pump exist some pneumatic purge valves which help the operator to eliminate the air bubbles. This operation is very important because the air bubbles can cause the breaking of the fiber in the coagulation bath. Due the high viscosity of the chitosan for its transport, a mechanical pump was used. At the exit of the pump a stainless-steel pipe is connected, which is immersed in the coagulation bath. At the end of the pipe a spinneret such as conical tube can be attached or just a silicon house for a fiber with big diameter. When the dope solution leaves the spinneret, it starts to coagulate, and a hydrogel cylinder is formed. The cylinder is caught with a tweezer and passed over a roller, in order to increase the residence time in the coagulation bath

The concentration of the dope chitosan solution was 2.5% (w/w) and the NaOH solution volume was close to 40 L and 1.5 M concentration. The fiber was drawn by a pulling roller with constant velocity 300 rph. The diameter of the roller was 6 cm. The coagulation time (the residence time of the fiber in the coagulation bath) was varied by modifying the fiber path inside the bath. An example is shown in the Fig. 2. The samples were taken in the point where the thread was leaving the coagulation bath, by cutting the cylinder with a scissor. Further, the non-coagulate chitosan solution from the sample was removed by using the compressed air. Finally, the chitosan thickness was measured using a microscope Olympus BX41, coupled with Olympus DP26 camera connected on-line at a PC. Several cross-section images are shown in Fig. 3.

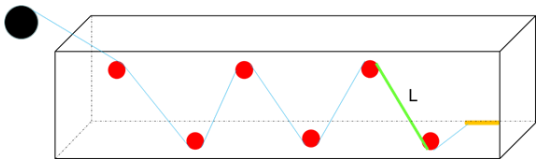

Fig. 2 An example of the fiber path in the coagulation bath; (L) the characteristic length used for calculus of the two dimensionless numbers.

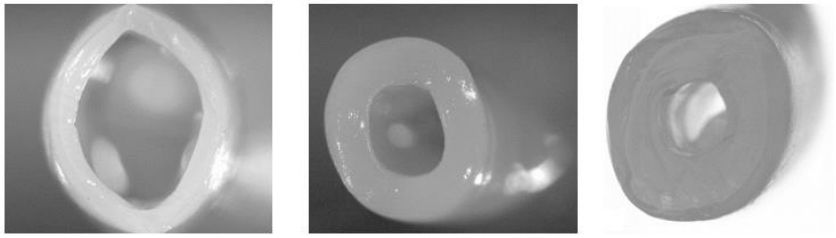

a) b) c)

Fig. 3 The propagation of the gel front in cylindrical filaments a) 35 s, b) 64 s, c) 96 s.

3. Mathematical model of the coagulation process

The development of the mathematical model of the coagulation process was performed using the following hypotheses:

- the neutralization reaction between the $-NH_3^+$ groups and NaOH is instantaneous [41], so that the step controlling the coagulation kinetics is the diffusion of NaOH trough the gel;
- the NaOH concentration at the gel / chitosan solution interface is negligible small;
- the concentration of sodium hydroxide inside the chitosan solution is null;
- the NaOH concentration in coagulation solution is approximated constant in time. This hypothesis is supported by the huge excess of NaOH into the aqueous solution and a value of NaOH diffusion coefficient in the aqueous solution slightly higher than that inside the gel volume.
- the NaOH diffusion coefficient is constant inside chitosan hydrogel.

The sodium hydroxide balance inside the chitosan gel is given by Fick's second law expression:

$$(1-\varepsilon)\cdot\frac{\partial C}{\partial t}=\frac{1}{r}\cdot\frac{\partial}{\partial r}\left(r\cdot D_{ef}\cdot\frac{\partial C}{\partial r}\right) \tag{2}$$

Initial condition and boundary condition (Fig. 4) are:

i) the absence of NaOH in the dope at the initial time:

$$\mathbf{t = 0,\ 0 \le r \le R,}\quad C(r,0) = 0 \tag{3}$$

ii) The NaOH flux continuity on the front interface:

$$\mathbf{t = 0,\ r = R,}\quad k_L\left(C_{sol} - C_i\right) = D_{ef}\,\frac{\partial C}{\partial r} \tag{4}$$

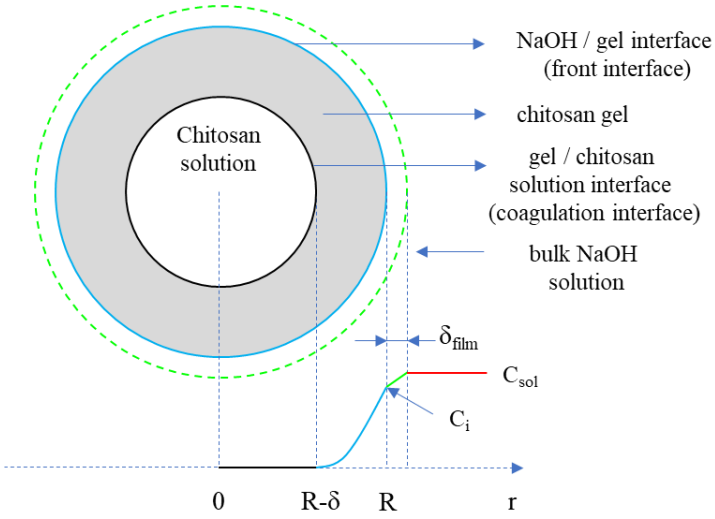

Fig. 4 Discretization of chitosan gel and non-coagulated chitosan solution.

iii) the consumption of NaOH is much faster than its transport by diffusion

$$\mathbf{t > 0,\ r = R - \delta,}\quad C(r,t) = 0 \tag{5}$$

The time evolution of gel thickness is calculated considering the stoichiometric relationship between the molar fluxes of NaOH and $-NH_3^+$ groups consumed at the coagulation interface, r=R-δ, defined by the equation:

$$\mathbf{t > 0,\ r = R - \delta,}\quad D_{ef}\,\frac{\partial C(r,t)}{\partial r} = \frac{\partial \delta}{\partial t} C_p n_{NH_2} \tag{6}$$

In the above equations: D_{ef} - diffusion coefficient of NaOH through the chitosan hydrogel, C - NaOH concentration in hydrogel, C_{sol} - NaOH concentration in bulk NaOH solution, C_i - NaOH concentration in liquid on the gel-solution interface, C_p - chitosan concentration in chitosan solution; K - NaOH partition coefficient, n_{NH2} - the number of $-NH_3^+$ groups/mole chitosan; ε - solid fraction, δ - the hydrogel thickness.

The coagulation model so defined was solved by using the method of lines. In this aim, the cylinder radius was divided into N-1 intervals, Δr. The spatial derivatives, appearing in equation (2), were discretized by the relations [42]:

$$\frac{\partial C_j}{\partial r} = \frac{C_{j+1} - C_{j-1}}{2\Delta r} \tag{7}$$

$$\frac{\partial^2 C_j}{\partial r^2} = \frac{C_{j+1} - 2C_j + C_{j-1}}{\Delta r^2} \tag{8}$$

In these equations, C_j represent the NaOH concentrations at points r_j, their time evolutions being calculated by numerical integration of equation (2), simultaneously with the equation (6), describing the evolution of hydrogel thickness. The integration of the ODE system was performed by using the 'ode45' function of the Matlab® programming environment.

A discontinuity is assumed on the gel interface between the equilibrium concentrations of NaOH in the two phases (C_1 and C_i), characterized by the partition coefficient defined by the relation:

$$K = \frac{C_1}{C_i} \tag{9}$$

As observed from our studies, the partition coefficient between NaOH solution and chitosan hydrogel is very close to unity, so we considered K≅1.

The value of NaOH concentration in the gel at r=R, C_1, was calculated from the boundary condition (4), where the derivative was approximated by the relation:

$$\frac{\partial C(0,t)}{\partial r} = \frac{C_1 - C_2}{\Delta r} \tag{10}$$

By substituting the equations (9) and (10) in the boundary condition (4), one obtains the equation:

$$C_1 = \frac{C_{sol} + \frac{D_{ef}}{\Delta r\, k_L} C_2}{1 + \frac{D_{ef}}{\Delta r\, k_L}} \tag{11}$$

The derivative $\frac{\partial C(r,t)}{\partial r}$ at r=R-δ, appearing in the equation (6) can be calculated by knowing a sequence of values C_n, C_{n-1}, C_{n-2}…at the points r_n, r_{n-1}, r_{n-2} ..., by using a polynomial interpolation method. This sequence is so chosen that $\delta \epsilon [r_n, r_{n-1})$. We used a second order polynomial interpolation over 4 points vicinal with the coagulation interface, C_n, C_{n-1}, C_{n-2}, C_{n-3}.

The difficulty in numerical solving of these equations resides in its initialization (obtaining of an initial NaOH concentration profile in a gel thickness of known value formed in a known coagulation time).

The adopted procedure is based on the hypothesis that the NaOH concentration in the gel interface with the NaOH solution is constant over a rather

short time interval (approximatively 10 seconds) at the beginning of the process and using the numerical method for the rest of the time. In these conditions, the NaOH concentration across the gel is approximated by the expression [43]:

$$C(x,t)=C_0\left[1-\frac{erf\left(\frac{x}{2\sqrt{D_{ef}t}}\right)}{erf\left(\frac{\delta}{2\sqrt{D_{ef}t}}\right)}\right];\ x=R-r;\ erf(y)=\frac{2}{\sqrt{\pi}}\int_0^y e^{-\lambda}d\lambda \tag{12}$$

With this approximation, the variation of the hydrogel thickness in time is given by the equation:

$$\frac{\partial\delta}{\partial t}=\frac{D_{ef}}{C_p n_{NH_2}}\frac{C_0\exp\left(-\frac{\delta^2}{4D_{ef}t}\right)}{\sqrt{\pi D_{ef}t}\,erf\left(\frac{\delta}{2\sqrt{D_{ef}t}}\right)} \tag{13}$$

Once an initializing profile was obtained from equations (12) and (13), the process evolution was calculated by numerical integration of equations (6) and (2), considering the time variation of NaOH concentration $C_1(t)$ at the interface between the gel and NaOH solution.

The effective sodium hydroxide diffusion coefficient inside the chitosan hydrogel, D_{ef}, was estimated by Enache et al. [44]. The mass transfer coefficient was determined using the Rotte correlation [45]. This correlation was obtained from mass transfer experiments occurring between a liquid and a continuous wire of nickel passing through a vertical recipient filled with $Fe(CN)_2$. As characteristic length in the definitions of the Sh and Pe numbers was chosen the height of the liquid in the recipient. The experimental data were correlated as the dependence betweeen Sherwood number and the square root of Peclet number given by the equation (14):

$$Sh=1.13\sqrt{Pe}\quad for\quad 4\cdot10^3<\sqrt{Pe}<4\cdot10^4\quad and\quad Sc>700 \tag{14}$$

$$Pe=\frac{UL}{D};\quad Sh=\frac{k_L L}{D} \tag{15}$$

where:U - fiber velocity, L - characteristic length (in our case is the distance between two pulling rollers in the coagulation bath (~ 20 cm), see the Fig .2; D - diffusion coefficient of NaOH in liquid, k_L- mass transfer coefficient,

The diffusion coefficient of the sodium hydroxide in liquid was calculated using the ions diffusivities and the averaging formula published by Cussler [47].

$$\frac{|z_1|+|z_2|}{D}=\frac{|z_2|}{D_1}+\frac{|z_1|}{D_2} \tag{16}$$

where $D_1= D_{Na}+=1.33\cdot10^{-9}$ $m^2\cdot s^{-1}$; $D_2= D_{HO}- =5.28\cdot10^{-9}$ $m^2\cdot s^{-1}$, $z_1=+1$ and $z_2 =-1$; one obtains the NaOH diffusion coefficient, $D=2.125\cdot10^{-9}$ $m^2\cdot s^{-1}$.

4. Results and discussion

The coagulation time, i.e. the residence time of the fiber in the bath was calculated from the length of its trajectory and the rotation speed of the pooling roller. The results are presented in Table 2. The length of the fiber trajectory was measured using a twine, at the end of the experiments.

Table 2.

Results from spinning plant.

Sample	Fiber length, cm	Coagulation time, seconds	Thickness (experimental), mm	Thickness (calculated), mm
1	55	35	0.600	0.499
2	100	64	0.650	0.696
3	127	81	0.720	0.789
4	150	96	0.900	0.865
5	166	106	0.840	0.911
6	180	115	1.050	0.950

The experimental data (the points) and the theoretical curves (solid lines) are presented in Fig. 5. The theoretical line was obtained for the diffusion coefficient value, $D_{ef}=1.035\cdot10^{-9}$ m^2/s [44]. The proposed coagulation model fits acceptable the experimental data. As can be observed, the first and last experimental points are overrated. This is experimental error can be associated with the idea that the measurements were not continuous (coagulation, cutting, removed the non-coagulated solution and finally measured under microscope) as in the case of the unidirectional diffusion [44]. The NaOH concentration profiles, inside the hydrogel, calculated at different coagulation times are given in Fig. 6. The NaOH concentration at the front interface is not constant, showing an increasing evolution in time, due the increasing of the gel resistance to the NaOH transport toward the coagulation interface, due to the increase of gel thickness. The increasing resistance of the gel thickness is inducing a decrease of NaOH flux and an increased NaOH concentration in the gel volume.

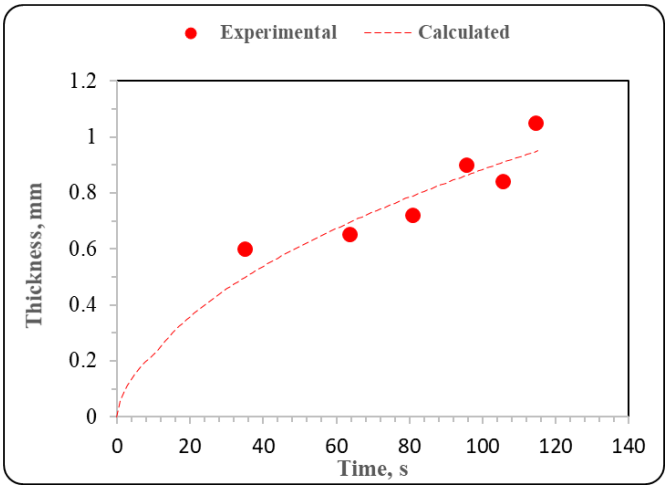

Fig. 5. Measured and calculated hydrogel thickness in time, for 2.5% chitosan and 1.5 M NaOH solution; ● - radial diffusion, samples tacked from spinning plant and measured under microscope; solid lines - calculated values using radial diffusion model (D_{ef}=1.035·10^{-9} m^2/s, k_L=1.49·10^{-5} m/s).

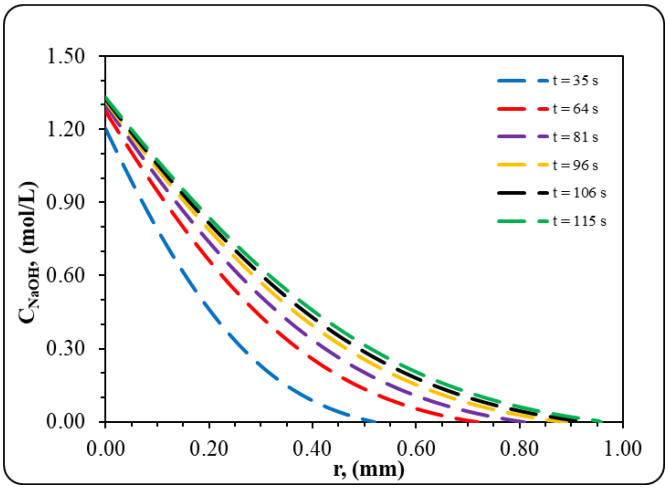

Fig. 6 NaOH concentration profiles inside the hydrogel (2.5 wt% chitosan and 1.5 M NaOH)

The value of the effective diffusion coefficient found for the experiments made on the pilot plant (1.035·10^{-9} m^2/s for a chitosan solution 2.5 % (w/v) and coagulated with 1.5 M NaOH) is placed between 1.05·10^{-9} m^2/s for a chitosan solution 2.5% (w/v) coagulated with 1 M NaOH and 1.00·10^{-9} m^2/s for a chitosan solution 2.5% (w/v) and coagulated with 4 M NaOH founded for the experiments in laboratory plant closer than the values for 1 M NaOH [44]. This implies that the

values of the diffusion coefficient determined in the laboratory plant can be used for scaling up experiments to the pilot plant. The value of the mass transfer coefficient derived from the relations (14) and (15) was of approximately $1.49 \cdot 10^{-5}$ m^2/s.

5. Conclusions

In the present study, the chitosan hydrogel coagulation experiments have been performed on a laboratory plant. The experiments allowed the determination of diffusion coefficients through the chitosan gel, using a modeling approach based on Fick second law. The calculated value of the effective diffusion coefficient was approximately $1.035 \cdot 10^{-9}$ m^2/s. Given that this value is between $1.05 \cdot 10^{-9}$ m^2/s obtained from experiments using a chitosan solution 2.5% (w/v) coagulated with 1 M NaOH and $1.00 \cdot 10^{-9}$ m^2/s calculated from experiments a chitosan solution 2.5 % (w/v) and coagulated with 4 M NaOH, it can be concluded that the diffusion coefficient determined in the laboratory plant can be used for scaling up experiments to the pilot plant.

The modelling and simulation study of the chitosan hydrogel wet-spinning described in this paper lead to an acceptable agreement with the measured data on a laboratory unit. This is proving that the proposed model can be used in the calculation of the coagulation step of the fiber formation process by wet spinning.

REFERENCES

[1] *A. Domard, M. Domard*, Chitosan: "Structure–Properties Relationship and Biomedical Applications". In: *Biomaterials*, S. Dimitriu, (Ed.), Marcel Dekker, New York, 2001, pp. 187.

[2] *E. Khor*, "Chitin: Fulfilling a Biomaterials Promise", Elsevier Science, Amsterdam, 2001.

[3] *M. H Ottoy., K. M. Vårum, O. Smidsrød*, "Compositional heterogeneity of heterogeneously deacetylated chitosans", in Carbohydrate Polymers, **vol. 29**, no. 1, 1996, pp. 17-24.

[4] *T. Sannan, K. Kurita, Y. Iwakura*, "Studies on chitin, 1. Solubility change by alkaline treatment and film casting", in Die Makromolekulare Chemie, **vol. 176**, no 4, 1975, pp. 1191-1195.

[5] *T. Sannan, K. Kurita, Y. Iwakura, "*Studies on chitin, 2. Effect of deacetylation on solubility", in Macromolecular Chemistry and Physics, **vol. 177**, no 12, 1976, pp 3589-3600.

[6] *S. Aiba*, "Studies on chitosan: 4. Lysozymic hydrolysis of partially N-acetylated chitosans", in Int. J. Biol. Macromol, **vol. 14**, 1992, pp. 225-228.

[7] *M. W. Anthonsen, K. M. Vårum, A. M. Hermansson, O. Smidsrød, D. A. Brant*, "Aggregates in acidic solutions of chitosans detected by static laser light scattering", in Carbohydr. Polym., **vol. 25**, no. 1, 1994, pp. 13-23.

[8] *S. Aiba*, "Studies on chitosan: 3. Evidence for the presence of random and block copolymer structures in partially N-acetylated chitosans", in Int. J. Biol. Macromol, **vol. 13**, 1991, pp. 40-44.

[9] *A. Anitha, S. Sowmya, P. T. Sudheesh Kumar, S. Deepthi, K.P. Chennazhi, H. Ehrlich, M. Tsurkan and R. Jayakumar*, "Chitin and chitosan in selected biomedical applications", in Progress in Polymer Science, **vol. 39**, no. 9, 2014, pp. 1644-1667.

[10] *F. Brunel, L. Véron, L. David, A. Domard, T. Delair*, "A Novel Synthesis of Chitosan Nanoparticles in Reverse Emulsion", in Langmuir, **vol. 24**, 2008, pp. 11370-11377.

[11] *M. Costalat, P. Alcouffe, L. David, T. Delair*, "Macro-hydrogels versus nanoparticles by the controlled assembly of polysaccharidesin", in Carbohyd Polym, **vol. 134**, 2015, pp. 541–546.

[12] *C. Halimi, A. Montembault, A. Guerry, T. Delair, E. Viguier, R, Fulchiron, L. David*, "Chitosan solutions as injectable systems for dermal filler applications. Rheological characterization and biological evidence", in 37th Annual Int. Conference of the IEEE, Eng. Med. Biol. Soc., Conference Proceedings **2015**, pp. 2596-2599; (http://ieeexplore.ieee.org/xpl/mostRecentIssue.jsp?punumber=7302811, accessed January 20, 2018).

[13] *S. Ladet, L.David, A. Domard*, "Multi-membrane hydrogels", in *Nature*, **vol. 452**, 2008, pp. 76-79,

[14] *H. Homayoni, S. Abdolkarim, H. Ravandi, M. Valizadeh*, "Electrospinning of chitosan nanofibers: Processing optimization", in Carbohyd Polym, **vol. 77**, 2009, pp. 656–661.

[15] *A. Osorio-Madrazo, L. David, C. Peniche-Covas, C. Rochas, J.-L Putaux, S, Trombotto, P. Alcouffe, A. Domard*, "Fine microstructure of processed chitosan nanofibril networks preserving directional packing and high molecular weight", in Carbohyd Polym, **vol. 131**, 2015, pp. 1–8.

[16] *L. Notin, C. Viton, L. David, P. Alcouffe, C. Rochas, A, Domard*, "Morphology and mechanical properties of chitosan fibers obtained by gel-spinning: influence of the dry-jet-stretching step and ageing", in Acta Biomater, **vol. 2**, 2006, pp. 387–402.

[17] *M. Desorme, A. Montembault, J. M. Lucas, C. Rochas, T. Bouet, L. David*, "Spinning of hydroalcoholic chitosan solutions", in Carbohyd Polym, **vol. 98**, 2013, pp. 50–63.

[18] *A. L. Andrady, P. Xu*, "Elastic behavior of chitosan films", in Polym Sci Pol Phys, **vol. 35**, 1997, pp. 517–521.

[19] *L. A Hadwiger*, "Plant science review: Multiple effects of chitosan on plant systems: Solid science or hype", in Plant Sci., **vol. 208**, 2013, pp. 42–49.

[20] *L. A. M. Van Den Broek., R. J. I. Knoop, F. H. J. Kappen, C. G. Boeriu*, "Chitosan films and blends for packaging material", in Carbohydr. Polym., **vol. 116**, 2015, pp. 237–242.

[22] *A. K. Patel*, "Chitosan: Emergence as potent candidate for green adhesive market", in Biochem. Eng. J., **vol. 102**, 2015, pp. 74–81.

[23] *F. Mohammad*, "Green Chemistry Approaches to Develop Antimicrobial Textiles Based on Sustainable Biopolymers-A Review", in Ind. Eng. Res., **vol. 52**, 2013, pp. 5245–5260.

[24] *A. Jimtaisong, N. Saewan*, "Utilization of carboxymethyl chitosan in cosmetics", in Int. J. Cosmet. Sci., **vol. 36**, 2014, pp. 12–21.

[25] *W. S. Wan Ngah, L. C. Teong, M. A. K. M. Hanafiah*, "Adsorption of dyes and heavy metal ions by chitosan composites: A review", in Carbohydr. Polym., **vol. 83**, 2011, pp. 1446–1456.

[26] *M. Dash, F. Chiellini, R. M. Ottenbrite, E. Chiellini*, "Chitosan - A versatile semi-synthetic polymer in biomedical applications", in Prog. Polym. Sci., **vol. 36**, 2011, pp. 981–1014.

[27] *R. Jayakumar, D. Menon, K. Manzoor, S. V. Nair, H. Tamura*, "Biomedical applications of chitin and chitosan-based nanomaterials - A short review", in Carbohydr. Polym., **vol. 82**, 2010, pp. 227–232.

[28] *R. A. A Muzzarelli*, "Chitins and chitosans for the repair of wounded skin, nerve, cartilage and bone", in Carbohydr. Polym., **vol. 76**, 2009, pp. 167–182.

[29] *F. Croisier, C. Jerome*, "Chitosan-based biomaterials for tissue engineering", in Eur. Polym. J., **vol. 49**, 2013, pp. 780–792.

[30] *V. Patrulea, V. Ostafe, G. Borchard, O. Jordan*, "Chitosan as a starting material for wound healing applications", in Eur. J. Pharm. Biopharm., **vol. 97**, 2015, pp. 417–426.

[31] *N. Bhattarai, J. Gunn, M. Zhang*, "Chitosan-based hydrogels for controlled, localized drug delivery", in Advanced Drug Delivery Reviews, **vol. 62**, 2010, pp. 83–99.

[32] *L. Casettari, L. Illum*, "Chitosan in nasal delivery systems for therapeutic drugs", in J. Control. Release, **vol. 190**, 2014, pp. 189–200.

[33] *A. Bernkop-Schnürch, S. Dünnhaupt*, "Chitosan-based drug delivery systems", in Eur. J. Pharm. Biopharm., **vol. 81**, 2012, pp. 463–469.

[34] *P. Agrawal P., G. J. Strijkers, K. Nicolay*, "Chitosan-based systems for molecular imaging", in Adv. Drug Deliv. Rev., **vol. 62**, 2010**,** pp. 42–58.

[35] *W. Suginta, P. Khunkaewla, A. Schulte*, "Electrochemical Biosensor Applications of Polysaccharides Chitin and Chitosan", in Chem. Rev., **vol. 113**, 2012, pp. 5458–5479.

[36] *J. Nie, Z. Wang, Q. Hu*, „Difference between Chitosan Hydrogels via Alkaline and Acidic Solvent Systems", in Nature Scientific Reports 6, Article number: 36053, 2016, doi:10.1038/srep36053.

[37] *M. Rinaudo*, "Chitin and chitosan: properties and applications", in Prog. Polym. Sci., **vol. 31**, 2006, pp. 603–632.

[38] *A. Chenite, M. Buschmann, D. Wang, C. Chaput, N. Kandani*, "Rheological characterisation of thermogelling chitosan/glycerol-poshphate solution", in Carbohydrate Polymers, **vol. 46**, 2001, pp. 39-47.

[39] *G. W. Rigby*, "Process for the preparation of films and filaments and products thereof", US Patent 2 040 880A, 19 May 1936**.**

[40] *B. C. Ming*, "Chitinfasern und chitosandruck", in Faserforsh Textiltech, **vol. 11**, 1960, pp. 320-326.

[41] *J. Z. Knaul, K A. M. Creber*, "Coagulation Rate Studies of Spinnable Chitosan Solutions", in Journal of Applied Polymer Science, **vol. 66**, 1997, pp. 117–127.

[42] *J. Kiusalaas*, "Numerical Methods in Engineering with Matlab", Cambridge University Press, Cambridge, 2005

[43] *C. K. Liu, J. A. Cuculo, B. Smith*, "Coagulation Studies for Cellulose in the Ammonia / Ammonium Thiocyanate (NH_3 / NH_4SCN) Direct Solvent System", in J. Polym. Sci. Polym. Phys. Part B., **vol. 27**, no. 12, 1989, pp. 2493-2511.

[44] *A. A. Enache, L. David, J,-P. Puaux, I. Banu, G. Bozga*, "Kinetics of chitosan coagulation from aqueous solutions", in Journal of Applied Polymer Science, **vol. 135**, no. 16, 2018, DOI:10.1002/app.46062

[45] *J. W. Rotte, G. L. J. Tummers, J. L. Dekker*, "Mass transfer to a moving continuous cylinder", in Chemical Engineering Science, **vol. 24**, 1969, pp. 1009-1015.

[46] *E. L. Cussler*, "Diffusion, Mass Transfer in Fluids Systems", 2nd ed., Cambridge University Press, Cambridge, 1997, pp.162, 166 and 237.